2016 13th International Conference on Ubiquitous Robots and Ambient Intelligence (URAI)
August 19~22, 2016 at Sofitel Xian on Renmin Square, Xian, China

Development of Underwater Terrain's Depth Map Representation Method based on Occupancy Grids with 3D Point Cloud from Polar Sonar Sensor System

Eon-ho Lee[1], Sejin Lee[1]
[1] Mechanical Engineering, Kongju National University, Chungnam, 330-710, Korea
(Tel : +82-41-521-9259; E-mail: sejiny3@kongju.ac.kr)

Abstract - This paper proposes the depth map representation method based on the occupancy grids by using 3D point cloud from the polar sonar sensor system. Because it is expensive to use current 3D sonar sensors, the low-cost 3D sensor systems are needed for the generalized purposes. So the polar-styled sonar sensor system was developed. It was constructed on the rotating motor with the 2D multi-beam sonar image sensor. And we developed the depth map model based on an occupancy probability grids map using the Bayesian-updating model. This way could reduce the noise caused by fundamental characteristics of a sonar sensor. The experiment was conducted to verify the validity and the usefulness of the proposed approach.

Keywords – Underwater sonar sensor, Terrain depth map, Bayesian rule, Occupancy grids, 3D point cloud.

1. Introduction

The year before last, in South Korea, a passenger ferry namely Sewol with 420 people has sunken into the ocean, and as a result, more than 300 people were dead. Over months, the government had a difficult time to search the bodies of those sacrificed. One of two main challenges were that the victims' bodies were washed away as time went by due to the strong current, and later it became really difficult to locate them due to the muggy water [1]. In 2013, a citizen committed a suicide by jumping from a bridge into the Han River which is running through Seoul, the capital city of South Korea, and is known for its muggy and fast running water. To recover the body of the citizen, a number of resources including a special purpose helicopter for over-the-water search-and-rescue operation were deployed. During the next 4 days, the search operation continued. However, the body was not recovered as it stayed mid-water and was not able to be seen from the rescuers outside the muggy water [2]. Based on the recent report on underwater searching equipment status by the national fire station, as of 2009, only 33 out of 2000 fire stations (1.44%) in South Korea possess a kind of underwater search-and-rescue equipment.

The importance of the exploring underwater has been increased due to above reasons. The existing (reasonable priced and thus widely used) equipment such as NAVIGATOR [3] suffers from an inherited physical restriction on the sonar as the user would recognize his/her surrounding within a reconstructed 2D space. On the other hand, the cost of high-end 3D sonar, e.g. ARIS Sonars of Sound Metrics, is so high that it is not practical to attach them to multiple robotic vehicles. Thus, providing 3D observability with underwater search equipment with 2D sonar sensor is of great practical value to construct the rapidly deployable system for searching mid-water human and objects. In this research, therefore, we plan to build the scanning sonar sensor equipment with M900-90 of TELEDYNE-BlueView to secure 3D observability and practicality. M900-90, 2D multi-beam imaging sonar, mounted on a motor would be rotated and synchronized together to take accurate 3D range point cloud data as shown in Fig. 1.

This paper proposes the depth map representation method to visualize underwater geographic features. The 3D point cloud achieved in underwater [4], [5] were refined by using the occupancy probability grids [6].

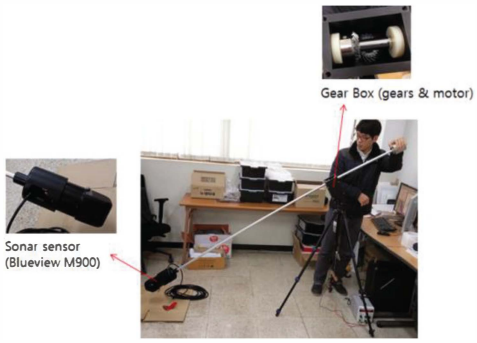

Fig. 1. Polar sonar sensor system with Blueview M900 and Dynamixel-Pro.

2. Model Architecture

Fig. 2 shows the flow chart of the proposed algorithm in this study. There are three steps such as achieving the 3D point cloud, creating the occupancy grid, and representing the depth map.

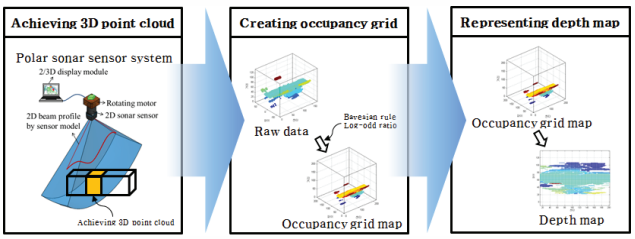

Fig. 2. The flow chart of the proposed algorithm.

2.1 Underwater sonar sensor

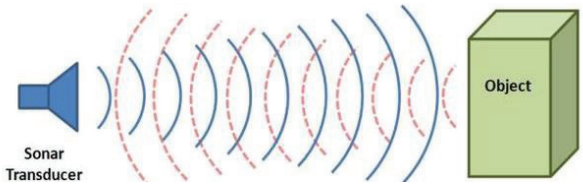

Fig. 3. A concept of a sonar senor.

A sonar sensor generates ultrasonic waves and it gets echoes as shown in Fig. 3. So, the sonar sensor has the retuned signals including a lot of ~~a~~ noise data caused by the reflection effect and the wide beam width. Therefore, the uncertainties of data set should be increased. Thus, this problem was handled by a stochastic method.

Table I. Specification of the Blueview M900.

Property	Capability
Frequency	900 (kHz)
Beam Width	1×20 (°)
Max. Range	1～100 (m)
Size	193×102×102 (mm)
Weight in Air	1,814 (g)
Supply Voltage	12-48 (V, DC)

2.2 Occupancy probability grids map algorithm

The occupancy probability grid mapping algorithm divides the space, and each grid is independent. It represents probability value about potential of an object. This value was calculated by (1) and (2). Equation (1) shows the Bayesian rule and (2) represents the log-odd ratio. The parameter, $p(m)$ is probability values for an each grid and $p(z)$ is the measurement value of the sensor in (1).

$$p(m_i|x_{1:t}, z_{1:t}) = \frac{p(m_i|x_t,z_t)p(z_t|x_t)}{p(m_i)} \frac{p(m_i|x_{1:t},z_{1:t-1})}{p(m_i|x_1,z_{1:t-1})} \quad (1)$$

$$\begin{aligned} \text{Odds}(m_i|x_{1:t}, z_{1:t}) &= l_t(m_i) \quad (2) \\ &= \log\frac{p(m|x_t, z_t)}{1-p(m|x_t, z_t)} + l_{t-1}(m_i) - l_0(m_i) \end{aligned}$$

2.2.1 Sensor model

The underwater sonar sensor model of the first term in (2) could be represented by (3) and (4) of the occupancy probability and the empty probability respectively. Equation (5) can be used for (3). The parameter, θ represents the rotating angle of the sensor system. The parameter, ϕ is the angle of each beam in the single 2D multi-beam sonar data. The parameter, z is the measured distance.

$$\begin{aligned} p_{occ,i} &= p_{occ}(\theta_i) \cdot p_{occ}(\phi_i) \cdot p_{occ}(z_i) \quad (3) \\ 0.5 &\le p_{occ,i} \le 1.0 \end{aligned}$$

$$\begin{aligned} p_{emp,i} &= p_{emp}(\theta_i) \cdot p_{emp}(\phi_i) \cdot p_{emp}(z_i) \quad (4) \\ 0 &\le p_{emp,i} < 0.5 \end{aligned}$$

$$\begin{aligned} p_{occ(\theta_i)} &= e^{\frac{-\theta^2}{2\sigma^2}}, 0 \le \theta \le 180 \\ p_{occ(\phi_i)} &= e^{\frac{-\phi^2}{2\sigma^2}}, -45 \le \phi \le 45 \quad (5) \\ p_{occ(z_i)} &= e^{\frac{-z^2}{2\sigma^2}}, 0 \le \theta \le 180 \end{aligned}$$

2.2.2 Polar coordinate

In this study, the polar coordinate in 3 dimensions can be represented by the measured distance, z in the vertical axis, the beam angle, ϕ in the y axis, and the rotation angle of a motor, θ counter-clockwise in the x axis as shown in Fig. 4.

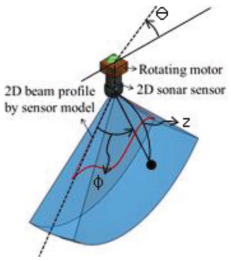

Fig. 4. Polar coordinate.

2.3 Depth map

The depth map could be represented by a color according to the measured distance, z of each grid. In this paper, the occupancy probability grids map as the depth map was built from 3D point cloud.

3. Experiments

Fig. 5. Polar sonar sensor system with USV.

Fig. 5 shows the polar sonar sensor system. It scaled down Fig. 2 for experiment. It could achieve 3D point cloud.

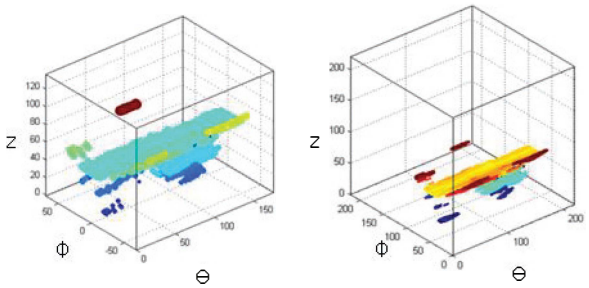

(a) 3D raw data

(b) Occupancy probability grids

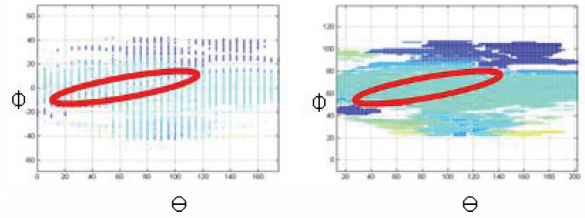

(c) Top view of raw data

(d) Depth map

Fig. 6. Raw data and processed data.

Fig. 6 (a) represented the 3D raw data of the 2D sonar sensor. Fig. 6 (b) was made of the 3D raw data by the occupancy probability grid. Fig. 6 (c) showed the raw data on the θ-ϕ plane. Fig. 6 (d) was the image data that represented the distance data by a color on the θ-ϕ plane. Red circles were shown in Fig. 6 (c) and (d). Blue dots marked by a red circle were showed in Fig. 6 (c). It was the noise data of the sonar sensor. But it was disappeared in Fig. 6 (d). This problem caused by the data noise was handled by the occupancy probability grids map algorithm. It renewed the each probability value of grids by the Bayesian updating rule. Then, this rule deleted the noise data.

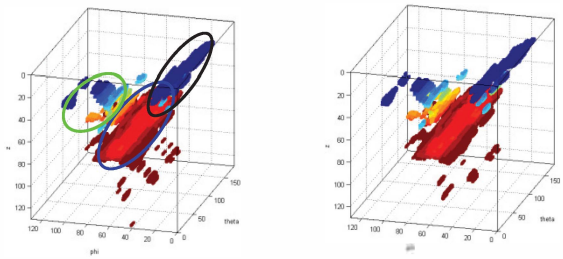

(a) USV Position 1

(b) USV Position 1

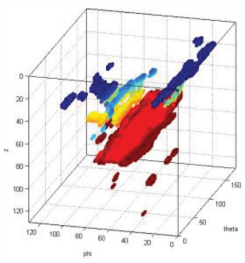

(c) USV Position 2

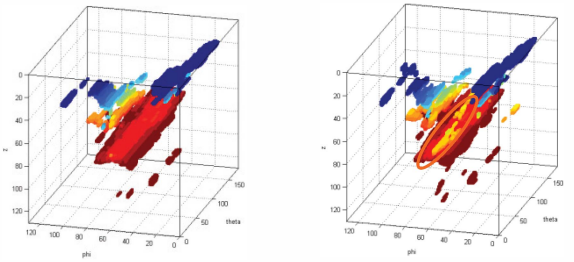

(d) USV Position1 & Cube Position 1

(e) USV Position1 & Cube Position 2

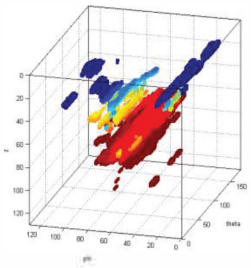

(f) USV Position 2 & Cube Position 2

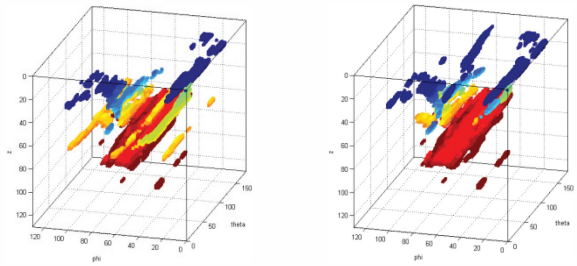

(g) USV Position 2 & Box Position 1

(h) USV Position 2 & Box Position 2

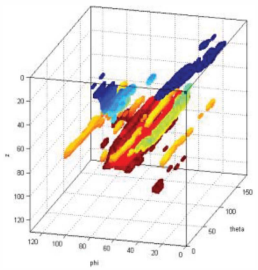

(i) USV Position 1 & Box Position 2

Fig. 7. Occupancy probability grids map of the real data.

Fig. 7 was made of the occupancy probability grids maps that created from the raw data to the occupancy probability grids map data. The 3D point cloud was achieved in a water tank. Their depth was 8(m). And 2 boxes were poured into a water tank for the experiment. Those size was 1(m)×1(m)×1(m) and 1(m)×1(m)×0.5(m). The USV., the cube and the box was moved when the 3D point cloud was achieved. In Fig. 7 (a), the green circle was meaning a structure in the water tank. The blue circle was meaning a floor in the water tank. The black circle was meaning a wall in the water tank. And the orange circle was meaning a cube or box at Fig. 7 (e). Fig. 7 (a), Fig. 7 (b) and Fig. 7 (c) were the occupancy probability grids map without the box or the cube. And the USV. was on the position 1 in Fig. 7 (a) and Fig. 7 (b). And the USV. lay on the position 2 in Fig. 7 (c). Fig. 7 (d), Fig. 7 (e) and Fig. 7 (f) were the occupancy probability grids map with the cube. And the USV. was on the position 1 in Fig. 7 (d) and Fig. 7 (e). The USV. lay on the position 2 in Fig. 7 (f). Then, the cube was on the position 1 in Fig. 7 (d). In Fig. 7 (e) and Fig. 7 (f), the cube lay on the position 2. Fig. 7 (g), Fig. 7 (h) and Fig. 7 (i) were the occupancy probability grids map with the box. And the USV. was on the position 2 in Fig. 7 (g) and Fig. 7 (h). The USV. lay on the position

1 in Fig. 7 (i). Then, the box was on the position 1 in Fig. 7 (g). In Fig. 7 (h) and Fig. 7 (i), the box lay on the position 2.

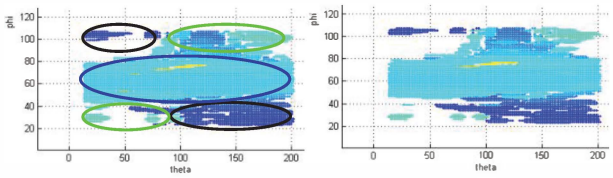

(a) USV Position 1 (b) USV Position 1

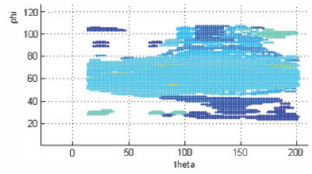

(c) USV Position 2

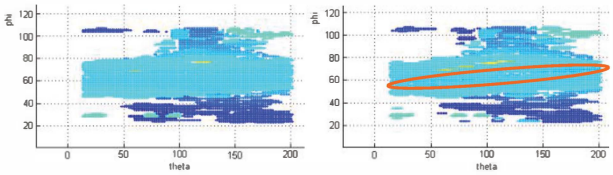

(d) USV Position 1 & Cube Position 1 (e) USV Position 1 & Cube Position 2

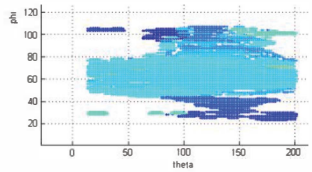

(f) USV Position 2 & Cube Position 2

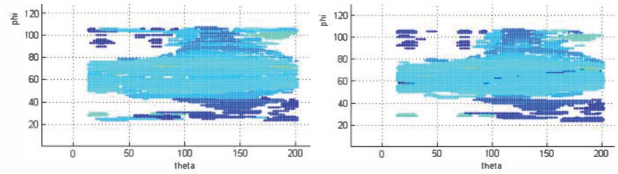

(g) USV Position 2 & Box Position 1 (h) USV Position 2 & Box Position 2

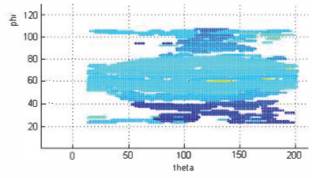

(i) USV Position 1 & Box Position 2

Fig. 8. Depth map of the real data.

Fig. 8 was made of depth maps that were created from the occupancy probability grids map data to the depth map data. As mentioned, the each green circle, blue circle, black circle and orange circle was a structure, a floor, a wall, a cube and a box. Fig. 8 (a), Fig. 8 (b) and Fig. 8 (c) were the depth map without the box or the cube. And the USV. was on the position 1 in Fig. 8 (a) and Fig. 8 (b). And the USV. lay on the position 2 in Fig. 8 (c). Fig. 7 (d), Fig. 7 (e) and Fig. 7 (f) were the depth map with the cube. And the USV. was on the position 1 in Fig. 8 (d) and Fig. 8 (e). The USV. lay on the position 2 in Fig. 8 (f). Then, the cube was on the position 1 in Fig. 8 (d). In Fig. 8 (e) and Fig. 8 (f), the cube lay on the position 2. Fig. 8 (g), Fig. 8 (h) and Fig. 8 (i) were the depth map with the box. And the USV. was on the position 2 in Fig. 8 (g) and Fig. 8 (h). The USV. lay on the position 1 in Fig. 8 (i). Then, the box was on the position 1 in Fig. 8 (g). In Fig. 8 (h) and Fig. 8 (i), the box lay on the position 2.

4. Conclusion

This paper proposed the depth map representation method based on the occupancy grids, because the future research will suggest a general pattern of underwater terrain features with the Deep Learning. Then, the Deep Learning used an image data more than a point clouds. So this paper proposed the representation method. But some problems were found. First, it's difficult to differentiate between the box or the cube and the floor. Second, did it need the process of converting from 3D point cloud to an image data? In fact, an image data was unrelated when the Deep Learning was trained. Just an image data was accessible in the previous research. So the efficiency and the usefulness should be verified between to study the Deep Learning by representing from 3D point cloud to the image data and to study the Deep Learning by 3D point cloud.

Acknowledgement

This research was supported by Basic Science Research Program through the National Research Foundation of Korea(NRF) funded by the Ministry of Science, ICT & Future Planning(NRF-2015R1C1A1A01054724).

References

[1] http://www.koreaherald.com/view.php?ud=20140501000824

[2] http://www.hani.co.kr/arti/english_edition/e_national/599060.html

[3] http://www.sharkmarine.com/Products/HandHeld/Nav.html

[4] SeJin Lee, "Representation of Underwater Terrain Shape based on 3D Point Cloud collected from Underwater Sonar Sensors", KRoC, 9, 1-4, 2014

[5] David Ribas, Pere Ridao, Jose Neira, "Underwater SLAM for Structured Environments Using an Imaging Sonar", Springer, 2010

[6] A. Elfes, "Occupancy grids: A probabilistic framework for robot perception and navigation", Ph.D. dissertation, CMU, 1989

[7] R. Socher, B. Huval, B. Bath, C. D. Manning and A. Y. Ng, "Convolutional-recursive Deep Learning for 3D Object Classification," In Advances in Neural Information Processing Systems, pp. 665-673, 2012.

[8] K. Jarrett, K. Kavukcuoglu, M. Ranzato and Y. LeCun, "What is the Best Multi-Stage Architecture for Object Recognition?," In IEEE 12th International Conference on Computer Vision, 2009, pp.2146-2153, 2009.